Magnetite Biomineralization in *Magnetospirillum gryphiswaldense*: Time-Resolved Magnetic and Structural Studies

M. Luisa Fdez-Gubieda,*,† Alicia Muela,‡ Javier Alonso,†,¶ Ana García-Prieto,§ Luca Olivi,∥ Rodrigo Fernández-Pacheco,⊥ and José Manuel Barandiarán†,¶

†Departamento de Electricidad y Electrónica, ‡Departamento de Inmunología, and §Departamento de Física Aplicada I, Universidad del País Vasco (UPV/EHU), Spain, ¶BCMaterials, Building No. 500, Technological Park of Biscay, Derio, Spain, ∥XAFS Beamline, Sincrotrone Trieste, Italy, and ⊥Laboratorio de Microscopías Avanzadas—Instituto de Nanociencia de Aragón (LMA—INA), Universidad de Zaragoza, Spain

ABSTRACT Magnetotactic bacteria biosynthesize magnetite nanoparticles of high structural and chemical purity that allow them to orientate in the geomagnetic field. In this work we have followed the process of biomineralization of these magnetite nanoparticles. We have performed a time-resolved study on magnetotactic bacteria *Magnetospirillum gryphiswaldense* strain MSR-1. From the combination of magnetic and structural studies by means of Fe K-edge X-ray absorption near edge structure (XANES) and high-resolution transmission electron microscopy we have identified and quantified two phases of Fe (ferrihydrite and magnetite) involved in the biomineralization process, confirming the role of ferrihydrite as the source of Fe ions for magnetite biomineralization in *M. gryphiswaldense*. We have distinguished two steps in the biomineralization process: the first, in which Fe is accumulated in the form of ferrihydrite, and the second, in which the magnetite is rapidly biomineralized from ferrihydrite. Finally, the XANES analysis suggests that the origin of the ferrihydrite could be at bacterial ferritin cores, characterized by a poorly crystalline structure and high phosphorus content.

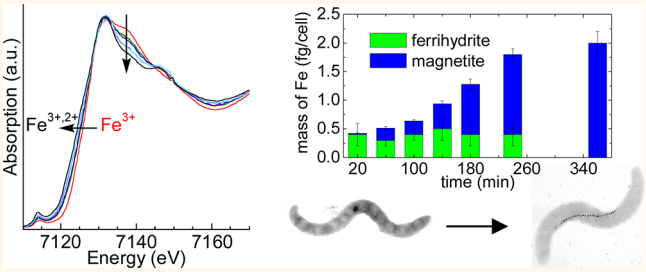

KEYWORDS: XANES · ICP–AES · TEM · HRTEM · XANES spectroscopy · magnetotactic bacteria · biomineralization · magnetic nanoparticles

Nature is a school for materials science and its associated disciplines such as chemistry and physics due to the ability to design crystalline structures whose properties are often superior to those of similar synthetic materials. The biologically controlled formation of inorganic compounds is called biomineralization. This process occurs in all organisms, from bacteria to humans. In particular, iron can be biomineralized in an Fe(III) oxyhydroxide phase, ferrihydrite, by an iron storage protein, ferritin. Some organisms biomineralize other iron oxides like goethite, α-FeOOH (limpets), lepidocrocite, γ-FeOOH (chiton)[1] and, the most common, magnetite, Fe_3O_4, that has been found in magnetotactic bacteria[2] and vertebrates such as pigeons, salmon, trout (see ref 3 and references therein) and even humans.[4]

In one particular case magnetotactic bacteria are able to mineralize magnetite nanocrystals with high chemical purity, species-specific crystal morphology on shape and size, and narrow size distribution. The magnetic nanoparticle is surrounded by a 3–4 nm thick lipid bilayer membrane with embedded proteins. The nanocrystal and its enveloping membrane comprise a magnetosome. The magnetotactic bacteria exert a highly precise biological control that determines the size, shape, and properties of the magnetite particles. These bacteria use these magnetosomes, which are organized in chains, as a compass needle that causes the bacteria to orient and navigate along the geomagnetic field lines.[5]

Although magnetotactic bacteria were first observed in 1963 by Bellini in Italy[6,7] and were introduced to the worldwide scientific

* Address correspondence to malu.gubieda@ehu.es.

Received for review December 27, 2012 and accepted March 26, 2013.

Published online March 26, 2013
10.1021/nn3059983

community in 1975 by Blakemore,[2] the interest in them has recently increased because of the potential biomedical applications of the magnetosomes.[8−11]

A good understanding of the biomineralization process is the key for addressing challenges as the design of new materials. In general, little is known about the biomineralization process of the bacteria, but several steps have been identified:[5] (i) magnetosome vesicles are formed,[12] (ii) iron is taken up from the environment, (iii) iron is transported into the magnetosome vesicle, and finally (iv) iron is nucleated and precipitated in the form of magnetite.

Different models have been proposed regarding this last step. First, by means of Mössbauer spectroscopy and transmission electron microscopy (TEM), Frankel *et al.*[13] suggest that magnetite is formed from a ferrihydrite precursor, which in a later work[14] is suggested to form an amorphous phase located on the surface of not fully developed magnetite particles. On the other hand, Faivre *et al.*,[15] using the same techniques in a time-resolved study, do not find evidence of the existence of a mineral precursor, and suggest as a possible mechanism of magnetite biomineralization a fast coprecipitation of Fe^{2+} and Fe^{3+} ions within the magnetosome vesicle, a hypothesis that was proposed earlier by Arakaki *et al.*[16] According to Faivre *et al.*,[15] these Fe^{2+} and Fe^{3+} ions would be converted into an intracellular ferrous high-spin species (Fe^{2+}) predominantly located in the membrane and into a membrane-associated ferritin (Fe^{3+}). The role of ferrihydrite as a source of Fe for magnetite biomineralization has also been suggested by Watanabe *et al.*[17] by means of Raman spectroscopy. A different mechanism is proposed by Staniland *et al.*[18] In this work, by means of X-ray absorption spectroscopy and X-ray magnetic circular dichroism on the soft Fe $L_{2,3}$-edges, they found a shell of an Fe oxide, hematite (α-Fe_2O_3), around the magnetite particles, which they suggest acts as the precursor of magnetite.

In the present work, we study the biomineralization process of the magnetotactic bacteria *Magnetospirillum gryphiswaldense* strain MSR-1 by the combination of magnetic and structural techniques in a time-resolved study. These techniques allow identification of two Fe phases during the process (magnetite and ferrihydrite) and, more importantly, measurement of the mass of each phase during the mineralization process. Besides more commonly used techniques like inductively coupled plasma-atomic emission spectroscopy (ICP−AES), magnetic analysis, and transmission electron microscopy (TEM), we have performed Fe K-edge X-ray absorption near edge structure (XANES) and high-resolution transmission electron microscopy (HRTEM).

The advantage of the XANES technique compared to those used in previous works, especially Mössbauer spectroscopy and soft X-ray absorption spectroscopy, is important. XANES is an element specific technique, sensitive to the oxidation state and to the local structure of the absorber element, in our case the Fe atom. Using hard X-rays at the Fe K-edge, instead of soft X-rays as in ref 18, allows us to work with the whole cell, avoiding the process of extraction of magnetosomes. Additionally, this technique is a powerful tool not only to identify but also quantify the different Fe inorganic phases present in the cell regardless of their magnetic state, which can be very complex and may mask magnetically weak phases as in Mössbauer spectroscopy or X-ray magnetic circular dichroism. It should also be noted that working with high doses of hard X-rays could damage a biological sample, especially metalloproteins in which an inorganic element is bound to organic ligands.[19,20] However, no damage should be expected in the inorganic phases present in the bacteria.

RESULTS AND DISCUSSION

Figure 1a shows a TEM image of *M. gryphiswaldense* with a fully formed magnetosome chain obtained after 72 h (4320 min) of incubation in a medium cointaining Fe(III)-citrate. *M. gryphiswaldense* synthesize cuboctahedral magnetite particles with an average diameter of 45 ± 3 nm and narrow size distribution of 8 nm (17%) (Figure 1b). The mean number of magnetosomes per cell ranges between 20 and 25,[21] which, assuming a mean particle size of 45 nm and a density of magnetite of 5.2×10^3 kg/m^3, gives an estimated mass of 4.9 to 6.2 fg of magnetite per cell. Electron microdiffraction on a single particle confirms that the magnetosomes are single crystals (Figure 1c). The magnetic response of the cells also corresponds to pure magnetite, as confirmed by the evolution of the magnetization as a function of temperature measured at 5 mT (Figure 2), which shows a sharp feature at 107 K that is due to the Verwey transition, a well-known characteristic of pure magnetite.[22] It should be noted that although this Verwey transition occurs at ~120 K in bulk magnetite, lower values (between 102 and 117 K) are found in magnetosomes,[23] a shift attributed to size effects. The presence of this sharp transition temperature together with the electron microdiffraction patterns are a clear indication of the high quality of the biogenic magnetite crystals obtained from the biomineralization process.

To follow the early stages of the biomineralization process of the bacteria, nonmagnetic cells ($t = 0$) were obtained after five passages in an iron-free medium, incubated under aerobic conditions. To induce the magnetite biomineralization, iron-starved cultures in midlogarithmic growth phase were harvested by centrifugation and the cells were transferred to fresh medium supplemented with 100 μM Fe(III)-citrate. At specific time intervals from $t = 20$ to 360 min, the cells were collected and fixed in 2% formaldehyde for

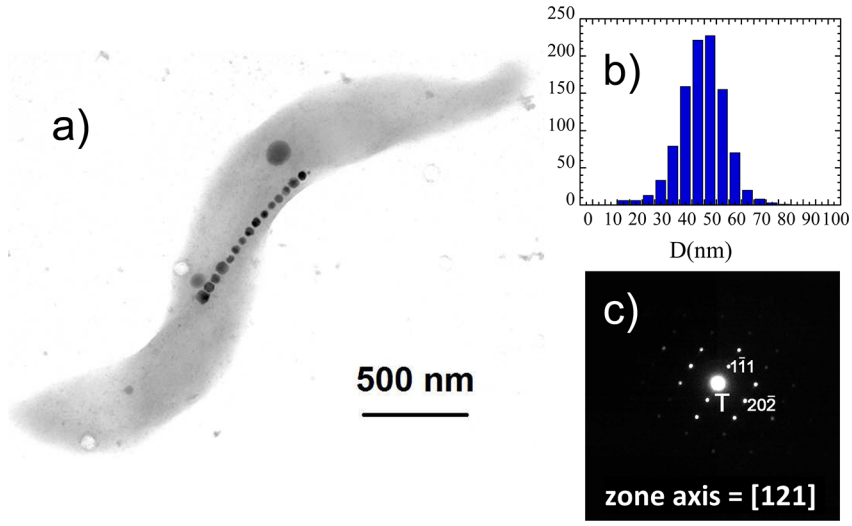

Figure 1. (a) TEM image of *Magnetospirillum gryphiswaldense* after 4320 min (72 h) of incubation in a medium containing Fe(III)-citrate. The chain of magnetosomes can be clearly observed. (b) Size distribution histogram and (c) microdiffraction pattern of a single magnetosome.

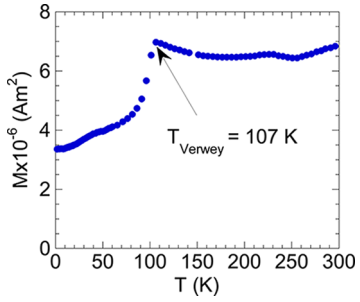

Figure 2. Magnetization versus temperature measured at 5 mT of *Magnetospirillum gryphiswaldense* after 4320 min (72 h) of incubation in a medium containing Fe(III)-citrate. The arrow marks the Verwey transition, characteristic of magnetite.

transmission electron microscopy (TEM) imaging, magnetic characterization, X-ray absorption near edge structure (XANES), and high resolution TEM (HRTEM). The cell-free culture medium left after cell harvesting was used for atomic emission spectroscopy (ICP−AES) measurements. The bacterial density at each time interval was monitored by counting the number of cells by the standard acridine orange procedure,[24] as specified in the Experimental section. This is an important point, as it will allow us to normalize every data to the number of cells. Finally, the magnetic response of the bacteria was monitored by an optical density method (see Figure 1 in the Supporting Information).

TEM images of the bacteria at specific times after Fe incubation allow the magnetosome mineralization process and the formation of magnetosome chains to be followed. In Figure 3 we present some TEM images with the corresponding size-distribution histograms that underline the main features found during the biomineralization process. The mean diameter ($\langle D \rangle$) and distribution width (σ) extracted from the histograms are presented in Table 1 together with the number of magnetosomes analyzed at each time. As shown in Figure 3, at increasing times after Fe incubation, the number and size of the nanoparticles increase. At early stages, t = 0−60 min, most of the bacteria do not present nanoparticles, and only occasionally some isolated nanoparticles can be observed. As the time after Fe incubation increases, the number of bacteria with nanoparticles does also increase. Most of these nanoparticles are isolated, but from t = 100 min, they organize in small "subchains" containing around 3−6 nanoparticles. With increasing time, these subchains become more frequent and closer together, and the size of the nanoparticles steadily increases. From t = 240 min, some long chains of several nanoparticles (>6) are formed by the union of these small subchains. From there on, the chains become longer, and formed by better defined and increasingly bigger nanoparticles. A similar evolution has been reported elsewhere.[25]

The mass of iron in the cell-free culture medium was followed by atomic emission spectroscopy (ICP−AES). These data together with the number of cells are plotted as a function of time after Fe incubation in Figure 2 in the Supporting Information. The difference between the ICP−AES measurement at t = 0 and at time t, normalized by the number of cells, gives indirectly a first estimation of the mass of iron taken up by the cells at a specific time t. The results of these measurements are shown in Table 2. According to these results, the mass of Fe per cell increases during the biomineralization process from 0.4 fg_{Fe}/cell at the beginning of the process up to 2.3 fg_{Fe}/cell at the end, that is, the mass of Fe per cell increases by a factor of 5. Regardless of the large indetermination associated with the measurements, from these data it can be inferred that this increment is not uniform but shows a change of slope at 140 min, slower before and faster after 140 min. As will be shown in the following, magnetic measurements and XANES show that the

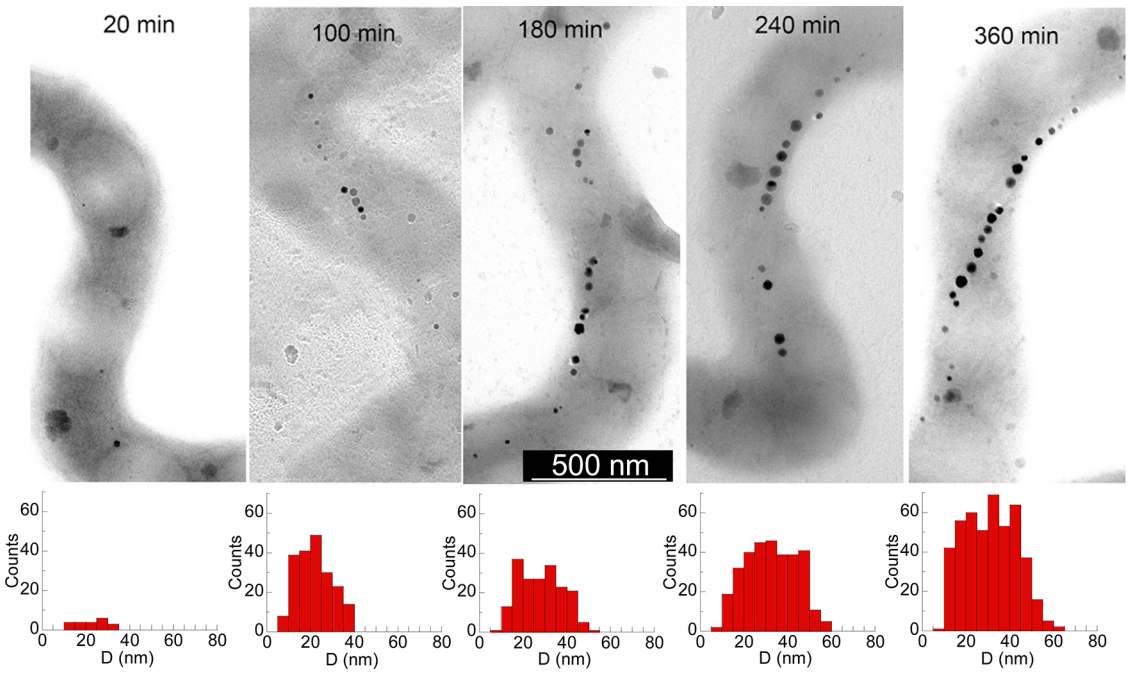

Figure 3. Time-resolved magnetosome and chain formation followed by TEM together with the corresponding size-distribution histograms. The mean diameter ($\langle D \rangle$) and distribution width (σ) extracted from the histograms are presented in Table 1.

TABLE 1. Mean Particle Size ($\langle D \rangle$) and Distribution Width (σ), Obtained from TEM Imaging (Figure 3). *N* is the Number of Magnetosomes Analyzed at Each Time after Fe Incubation

t (min) =	20	60	100	140	180	240	360
$\langle D \rangle$ (nm)	22.4	26.0	22.0	25.8	27.9	26	31.2
σ (nm)	6.6	10.5	7.7	8.3	9.6	8	11.6
N	21	84	204	184	189	319	456

TABLE 2. Total Mass of Fe (m_{Fe}), Fe in Magnetite ($m_{Fe,magnetite}$), and Fe in Ferrihydrite ($m_{Fe,ferrihydrite}$) (in fg/cell)[a]

technique	*t* (min) =	20	60	100	140	180	240	360
ICP—AES	m_{Fe}	0.4(2)	0.6(2)	0.3(2)	0.6(2)	1.0(2)	1.8(3)	2.3(3)
MH-XANES	m_{Fe}	0.4(2)	0.5(1)	0.6(1)	0.9(2)	1.3(2)	1.8(2)	2.0(3)
MH	$m_{Fe,magnetite}$	0.02(1)	0.21(3)	0.24(2)	0.44(5)	0.88(9)	1.4(1)	2.0(2)
MH-XANES	$m_{Fe,ferrihydrite}$	0.4(2)	0.3(1)	0.4(1)	0.5(2)	0.4(2)	0.4(2)	0.0(2)

[a] Values obtained by the following techniques at specific times after Fe incubation (*t* (min)): ICP—AES, magnetic measurements (MH), and the combination of magnetic and XANES measurements (MH-XANES). A detailed calculation of these data together with the associated errors can be found in the Supporting Information.

Fe taken up by the cells is distributed in two Fe compounds: magnetite and ferrihydrite.

The mass of magnetite per cell at specific times after Fe incubation has been determined by means of magnetic measurements. This magnetic analysis consisted of measuring the room-temperature hysteresis loops of bacteria at each time *t*. As will be shown below, these magnetic measurements have allowed us to assess how the mass of magnetite increases with the time after Fe incubation, and also to quantify the mass of magnetite per cell. This is because the ferrimagnetic signal of magnetite is much larger than any other in the samples and easily reaches magnetic saturation. On the other hand, the other magnetic signals, present in the samples, evolve linearly with the applied magnetic field at room temperature (diamagnetic signal from the organic parts and the sample holder and antiferromagnetic or weakly superparamagnetic from the ferrihydrite phase that will be analyzed further in the next paragraphs) and can be easily subtracted from the experimental data.

The hysteresis loops at several time points are shown in Figure 4 after subtraction of the linear magnetic contribution mentioned above. From the saturation magnetization of the loop, M_s, and the number of cells per sample, we have estimated the mass of magnetite per cell, taking into account that M_s for bulk magnetite is 92 Am^2/kg. The results show that at the first stages of the biomineralization process, $60 \leq t \leq 100$ min, the mass of magnetite per cell is very small ($\leq 0.30 \pm 0.04$ $fg_{Fe_3O_4}$/cell), but increases quickly up to 2.9 ± 0.1 $fg_{Fe_3O_4}$/cell for $t = 360$ min. This value is still lower than the mass of magnetite estimated previously for bacteria with fully formed magnetosome chains (4.9 to 6.2 $fg_{Fe_3O_4}$/cell), indicating that the biomineralization process is not yet complete at 360 min. These data are included in Table 2 in terms of mass of Fe in magnetite phase per cell. At this point, it should be noted that even though magneto-optical density of the cultures

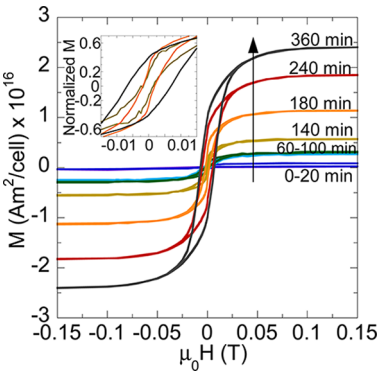

Figure 4. Hysteresis loops (after removal of the linear magnetic contribution) measured at room temperature at every *t* after Fe incubation. In the inset the shape of the hysteresis loop at low fields is depicted.

at $t = 0$ and $t = 20$ min is zero ($C_{mag} = 0$) (see Figure 1 in the Supporting Information), magnetic measurements by means of room-temperature hysteresis loops reveal a barely measurable magnetic signal (only 5% of the total mass of Fe per cell according to ICP−AES measurements, see Table 2), an indication of the presence of a few isolated magnetite particles as shown previously in the TEM images.

Additionally, at low magnetic field values, the hysteresis loops present a butterfly shape that disappears at $t \geq 240$ min. The origin of this butterfly shape is attributed to the coexistence of unblocked (superparamagnetic) and blocked ferrimagnetic magnetite nanoparticles. In fact, the contribution of smaller (superparamagnetic) magnetite nanoparticles is important at the first stages of the biomineralization process, but this contribution is masked by the prevalence of bigger (blocked) particles at later stages of the process.

To identify the different Fe phases present in the bacteria at specific times after Fe incubation, we have performed Fe K-edge X-ray absorption near edge structure (XANES) experiments at the XAFS beamline of the Elettra Synchrotron (Italy).

Figure 5 shows an evolution of the XANES spectra during the biomineralization process at energies below the edge, at the edge (7112 eV), and above the edge.

At early stages of the biomineralization process, the Fe K-edge XANES spectra show a shoulder, at around 14 eV below the edge, that transforms into a well-defined peak at the last stages of the biomineralization process. This pre-edge peak corresponds to a 1s to 3d transition, forbidden by the dipole selection rules. The intensity and width of this peak is sensitive to the symmetry around the absorbing atom.[26] The change of the pre-edge peak with the time elapsed after Fe incubation reflects a change on the symmetry around the Fe atoms, from a centrosymmetric (broad and low in intensity pre-edge peak) to a noncentrosymmetric site (narrow and more intense pre-edge peak).

The edge position is a clear-cut indication of the oxidation state of the absorbing atom, Fe in this case. In

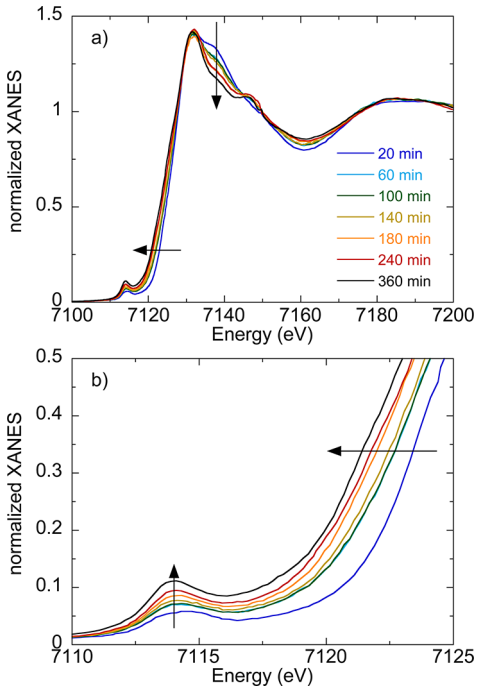

Figure 5. (a) Normalized XANES spectra at Fe K-edge obtained for the samples at specific times after Fe incubation; (b) pre-edge region in a more-detailed depiction.

fact, we have checked that the edge position displaces 7 eV to lower energies when the oxidation state decreases from Fe^{3+}, measured for reference compounds γ-Fe_2O_3 (maghemite) and Fe(III)-citrate, to Fe^{2+}, measured for the reference compound FeO (Figure 3 in the Supporting Information). The edge position of the first bacterial sample, $t = 20$ min, is coincident with a pure Fe^{3+} compound. As the biomineralization process evolves, the energy of the absorption edge displaces ~2 eV to lower energies, indicating that the Fe is reducing as the process evolves, from Fe^{3+} to the presence of both Fe^{3+}, Fe^{2+} oxidation states whose relative amount changes with the time elapsed after Fe incubation. It is well-known that magnetite (Fe_3O_4) is an inverse spinel in which 8 Fe^{3+} occupy the noncentrosymmetric tetrahedral sites and 8 Fe^{2+} and 8 Fe^{3+} occupy the centrosymmetric octahedral sites. Therefore, both features, the appearance of the pre-edge peak and the shift of the edge position, are evidence of the magnetite being formed from a pure Fe^{3+} compound.

Finally, above the edge, the XANES spectra evolve progressively with increasing time after Fe incubation. The main feature is the evolution of a shoulder observed at ~7136 eV that disappears as the process goes on. The evolution of the oscillations above the edge indicates that the surroundings of the Fe atoms change during the biomineralization process.

To obtain quantitative information on the different phases present in the cells and their evolution with the time elapsed after Fe incubation, the normalized spectra were fitted to a linear combination of two reference

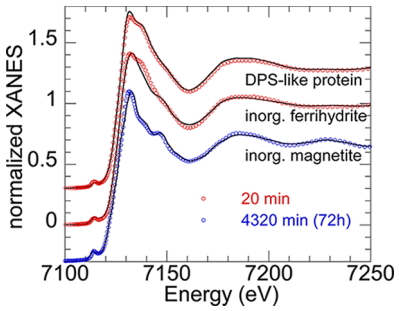

Figure 6. Comparison of the XANES spectra of bacteria at t = 20 min after Fe incubation with inorganic ferrihydrite and with *Streptococcus suis* DPS-like peroxide resistance protein (provided by A. Kauko and A.C. Papageorgiou[28]), and bacteria at t = 4320 min (72 h) with inorganic magnetite.

compounds. The percentage of each phase is the atomic fraction of the two phases present in the sample.

The first reference compound is the iron material in the bacteria at t = 20 min, which according to previous TEM and magnetic measurements is essentially free of magnetite (only 5% of the total mass of Fe, see Table 2). In fact, as noted before, the edge position of this spectrum corresponds to a pure Fe^{3+} compound, and comparing this spectrum with those of Fe^{3+} inorganic compounds such as hematite (α-Fe_2O_3), maghemite (γ-Fe_2O_3), goethite (α-FeOOH), Fe(III)-citrate, lepidocrocite (γ-FeOOH), and ferrihydrite, we found that it can be clearly identified as a ferrihydrite-like structure (Figure 6). However, the bacterial spectrum presents a shoulder at ~7136 eV that is not present in the ferrihydrite spectrum. This shoulder appears in ferrihydrite cores of ferritin proteins with high phosphorus content, such as plant ferritins[27] or bacterial ferritin-like proteins.[28] In fact, in bacterial ferritins the phosphorus content can be as high as 100% that of Fe.[29] The fact that the XANES spectrum of the sample at 20 min could correspond to a phosphorus-rich ferrihydrite is supported by Figure 6, where the good agreement between the XANES spectra of the sample at 20 min and the bacterial ferritin-like protein peroxide resistance protein in *Streptococus suis* (ref. 28) can be observed. Because of these special features of bacterial ferrihydrite as compared to inorganic ferrihydrite, the spectrum of the bacteria at t = 20 min was chosen as a reference compound for bacterial ferrihydrite for the rest of the samples. However, it should be noted that even though there is a small quantity of magnetite in these bacteria at t = 20 min, introducing magnetite in the XANES fit does not improve its quality. Moreover, introducing up to a 10% of magnetite in the fit only shifts the edge position by 0.2 eV, which is below the resolution limit of our XANES measurements (0.3 eV).

The second reference compound corresponds to the bacteria with fully formed magnetosome chains (t = 4320 min (72 h)). A comparison of this spectrum with the one of bulk magnetite shows that both are identical (Figure 6). However, a ferrihydrite content up to 10% could be present owing to the resolution limit of the experiment, as noted above.

TABLE 3. Atomic fraction of Bacterial Ferrihydrite (Bacteria at t = 20 min) and Biogenic Magnetite (t = 4320 min (72 h)) as Obtained from the Linear Combination of XANES Spectra at Every t after Fe Incubation

t (min) =	20	60	100	140	180	240	360
ferrihydrite	1.0(1)	0.6(1)	0.6(1)	0.5(1)	0.3(1)	0.2(1)	0.0(1)
magnetite	0.0(1)	0.4(1)	0.4(1)	0.5(1)	0.7(1)	0.8(1)	1.0(1)

The spectra of the bacteria at specific times after Fe incubation were then fitted to a linear combination of both biogenic references, ferrihydrite (t = 20 min) and magnetite (t = 4320 min (72 h)). As a result of these fits we have been able to quantify the atomic fraction of ferrihydrite and magnetite at each time after Fe incubation, as shown in Table 3. From these data it can be readily seen that at the beginning of the biomineralization process mostly ferrihydrite is present in the cells, which transforms progressively to magnetite as the process evolves.

From the atomic fraction of bacterial ferrihydrite and magnetite as determined by XANES (Table 3), and the mass of magnetite obtained from the saturation magnetization value M_s of the hysteresis loops (MH in Table 2), the mass of ferrihydrite per cell has been determined by means of the following equation:

$$m_{\text{Fe, ferrihydrite}} = \frac{1-\alpha}{\alpha} m_{\text{Fe, magnetite}} \qquad (1)$$

where α is the atomic fraction of Fe in the magnetite phase, and $m_{\text{Fe,ferrihydrite}}$ and $m_{\text{Fe,magnetite}}$ are the mass of Fe in the ferrihydrite and in the magnetite phases, respectively. These data, together with the total mass of Fe per cell ($m_{\text{Fe}} = m_{\text{Fe,ferrihydrite}} + m_{\text{Fe,magnetite}}$), are presented in Table 2 and in Figure 7.

In Figure 7a the data for the total mass of Fe per cell have been plotted together with the data obtained indirectly by ICP–AES. Despite some differences in the absolute values obtained by both independent techniques, mainly attributed to the rough estimation of the ICP–AES measurement, it is remarkable the similar overall evolution of the Fe content with incubation time resulting from both measurements. This supports the idea of the biomineralization process taking place in two well-distinguished rates: at the beginning of the biomineralization process, up to 140 min, the Fe content increases only very slowly, but after this point the rate of increase becomes larger, being in this second stage of the process where most of the overall increment in the Fe content takes place.

Furthermore, in Figure 7b we have represented the mass of Fe per cell in the form of both ferrihydrite and magnetite at each time after Fe incubation. These results show that up to t = 140 min, in the slow stages of the

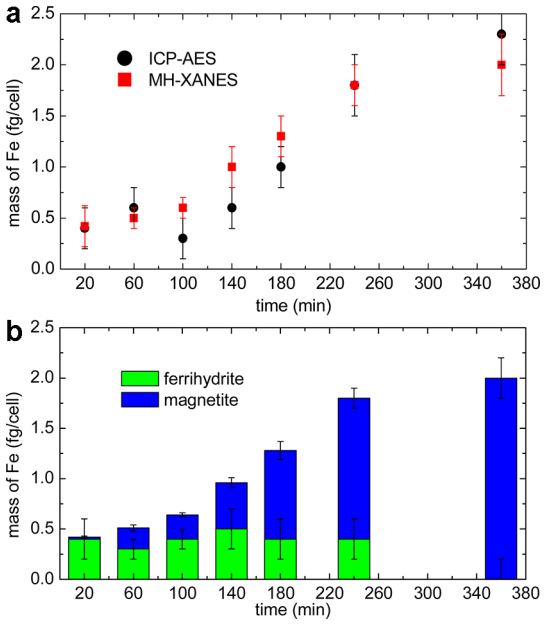

Figure 7. (a) Mass of Fe per cell as determined by ICP–AES and by a combination of XANES and magnetic measurements (MH) (Table 2). (b) Distribution of the mass of Fe per cell in the ferrihydrite and magnetite phases as determined by the combination of magnetic and XANES results.

process, the mass of ferrihydrite per cell remains practically constant, suggesting that in these stages the accumulation of Fe in the form of ferrihydrite prevails over the biomineralization of magnetite. Second, after t = 140 min, the biomineralization process of magnetite becomes faster and the mass of ferrihydrite decreases, until at 360 min it becomes undetectable by XANES, which for the sample at 360 min means less than 0.2 fg_{Fe}/cell. This suggests that ferrihydrite is progressively being transformed into magnetite but is not being replaced, thus one-third of the Fe atoms of ferrihydrite are being reduced to Fe^{2+}.

The question arising at this point is in which cellular compartment the bacteria store the ferrihydrite they use as a source of Fe and which, according to XANES results, is likely to be forming the cores of bacterial ferritin proteins.

To shed light on this matter, we have performed high resolution TEM experiments using a TITAN3 (FEI) microscope at the Instituto de Nanociencia de Aragón, Spain. These experiments were performed on the bacterial sample at t = 20 min after Fe incubation, in which, according to our previous results, the Fe is mainly forming ferrihydrite.

HRTEM images of bacteria at t = 20 min show very few isolated particles, always larger than 9 nm in size (see Figure 8), crystallized in the magnetite (Fe_3O_4)

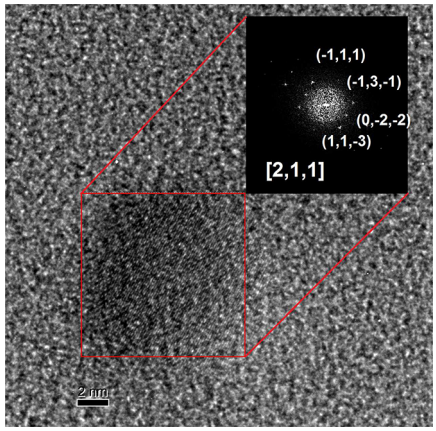

Figure 8. HRTEM image of an isolated nanoparticle from the t = 20 min bacterial sample The inset shows the diffractogram of the magnetite nanoparticle inside the bacteria.

phase. The crystalline structure has been determined from the indexation of the diffraction spots (see the inset of Figure 8), which yields a magnetite structure oriented in the [2,1,1] zone axis.

HRTEM observations did not reveal the presence of ferrihydrite in the samples. However, it should be noted that ferrihydrite cores from bacterial ferritin proteins have a very low density because of their high phosphorus content[29] and a low degree of crystallinity. For these reasons they present a very poor diffraction contrast in HRTEM,[30] which could explain why we have not been able to image them.

CONCLUSION

We have performed a time-resolved study on the biomineralization process of the magnetotactic bacteria *Magnetospirillum gryphiswaldense* strain MSR-1 combining structural and magnetic techniques. XANES allows identifying two Fe phases present in the bacteria: ferrihydrite with a similar structure and high phosphorus content as that of bacterial ferritin cores, and magnetite. This confirms the role of ferrihydrite as a source of Fe for the magnetite biomineralization. Additionally, we have been able to quantify the mass of each phase at specific times after Fe incubation, distinguishing two steps in the biomineralization process: the first, in which Fe is accumulated in the form of ferrihydrite, and the second, in which the magnetite is rapidly biomineralized from ferrihydrite. HRTEM confirms that even the smallest and not fully grown particles observed, of ~9 nm, are pure crystalline magnetite and rules out the coexistence of a crystalline–amorphous interface as suggested elsewhere.[13]

EXPERIMENTAL SECTION

Bacterial Strain and Growth Conditions. The bacteria studied in this work were *Magnetospirillum gryphiswaldense* strain MSR-1 (DMSZ 6631). *M. gryphiswaldense* was cultured in a flask standard medium (FSM) described by Heyen & Schüler[31] (per liter of deionized water: 0.1 g of KH_2PO_4, 0.15 g of $MgSO_4 \cdot 7H_2O$, 2.38 g of Hepes, 0.34 g of $NaNO_3$, 0.1 g of yeast extract, 3 g of soy bean peptone). The medium contained 0.3% (wt/vol) sodium

pyruvate as a carbon source. When needed, Fe(III)-citrate was added at a final concentration of 100 μM. Cells were grown at 28 °C without agitation in loosely stoppered bottles with a headspace-to-liquid ratio of approximately 1:4 and air was used in the headspace. An inoculum of 10% of the culture volume was used. Microaerobic conditions arose in the medium at higher cell densities by oxygen consumption of cells. Bacterial growth and magnetic response of the cells were monitored turbidimetrically at 565 nm (OD_{565}). For the magneto-optical density measurements, C_{mag}, two bar magnets (neodymium iron boron) were placed into the sample holder to create a magnetic field ($\mu_0 H = 20$ mT) parallel and perpendicularly to the incident light beam. The ratio of the resulting maximum and minimum OD values minus 1 ($C_{mag} = (OD_{\parallel}/OD_{\perp}) - 1$) can be used as a rapid qualitative estimation of magnetite formation. Thus, $C_{mag} = 0$ was obtained for nonmagnetic cells; this value increases with increasing magnetosomes and chain formation.[32]

Time-Course Experiments. To follow the early stages of magnetite synthesis, nonmagnetic cells were obtained after 4 or 5 passages in a free-iron medium incubated under aerobic conditions (shaking at 170 rpm). For induction of magnetite biomineralization, iron starved cells in midlogarithmic growth phase were harvested by centrifugation and transferred to fresh medium supplemented with 100 μM Fe(III)-citrate. To minimize the effect of physicochemical gradients generated in big flasks, the experiment was performed in eight separate 60 mL-flasks with 50 mL-subsamples of the same Fe-culture. The entire subsample was processed each time. Culture was carried out at 28 °C under microaerobic conditions (without agitation). At specified time intervals, samples were collected and fixed in 2% formaldehyde for subsequent analysis.

The evolution of the bacterial number throughout the experiment was followed by direct count of cells under fluorescence microscope by the standard acridine orange procedure.[24] Bacteria were retained on 0.22 μm pore-size black polycarbonate filters and examined under epifluorescence microscopy. These data were used to normalize the results of iron uptake and magnetic characterization by the number of cells.

The mass of Fe in the cell-free culture medium was determined by ICP−AES. The samples were centrifuged (6000 rpm, 20 min), and the supernatants were decanted, acidified to pH 2−3 with nitric acid, and analyzed directly. The iron taken up by the cell at each time after Fe incubation, t, was determined by subtraction of the iron in the supernatant at $t = 0$ and the one obtained at time t. Finally, the mass of iron was normalized by the total number of cells.

Transmission Electron Microscopy (TEM) and High-Resolution TEM (HRTEM). Electron microscopy was performed on unstained cells adsorbed onto 300 mesh carbon-coated copper grids.

TEM images were obtained with a Philips EM208S electron microscope at an accelerating voltage of 70 kV. The particle size distribution was analyzed using standard software for digital electron microscope image processing, ImageJ.[33] Electron microdiffraction was performed on a Philips CM200 electron microscope at an accelerating voltage of 200 kV and with an electron beam size of 40 nm.

High-resolution TEM (HRTEM) images were taken at a TITAN3 (FEI) microscope, working at 300 kV. This ultra-high-resolution microscope is equipped with a SuperTwin objective lens and a CETCOR Cs-objective corrector from CEOS Company allowing a point to point resolution of 0.08 nm. Correction of the spherical aberration of the objective lens improves significantly the spatial resolution of the HRTEM images.

Magnetic Characterization. The room temperature hysteresis loops of the samples of the time-resolved experiment were measured using a vibrating sample magnetometer (VSM) up to a maximum applied field of 1 T. For these measurements cells were collected by centrifugation at 4 °C and 6000 rpm for 15 min. The obtained pellets were then washed three times with 10 mM Hepes, pH 7.4, and were measured in the VSM in an Eppendorf holder. The magnetic signal (in Am^2) was normalized by the number of cells to obtain Am^2/cell.

The magnetic characterization of bacteria with fully formed magnetosome chains ($t = 4320$ min (72 h)) was carried out in a SQUID magnetometer (Quantum Design, MPMS-7). Bacterial pellets were left to dry at 37 °C for the SQUID measurement, which consisted of a zero-field-cooling curve: the sample is cooled from room temperature down to 5 K, without applied magnetic field, and then a magnetic field of 5 mT is applied. Afterward, the magnetization is measured while the sample warms to room temperature.

X-ray Absorption Near Edge Structure (XANES). Experiment and Sample Preparation. For the X-ray absorption near edge structure (XANES) experiments the same pellets used for the magnetic characterization were deposited onto Kapton foil and left to dry at a maximum temperature of 37 °C in order to prevent any inorganic phases present in the samples to be modified. The Kapton foil had been adhered to a sample holder specially designed to concentrate the sample in thin disks of ~28 mm^2.

XANES measurements were performed at the XAFS beamline of the Elettra Synchrotron in Trieste, Italy. The maximum flux in the beamline is of 3×10^9 ph/s at 7 keV. The beam size was of 1×2 mm^2 with the exposure time per spectrum of 40 min, which results in an X-ray dose of 3.6×10^6 ph/μm^2, lower than 10^7 ph/μm^2, which should not damage the biological samples[19] nor the inorganic phases in which we are interested. To improve the data reliability, between 3 and 6 spectra were recorded for each sample. We could check that the signal from every successive scan was invariant as a proof of the samples being intact after X-ray irradiation.

Room temperature Fe K-edge XANES spectra of bacteria at specific times after Fe incubation were recorded simultaneously in transmission and fluorescence mode with a single-element solid-state detector. For the subsequent analysis, the fluorescence spectra were used for the samples with low Fe contents, but for higher Fe contents where autoabsorption mechanisms were important, the transmission spectra were used.

The monochromator used in the experiments was a double crystal of Si(111). The energy edge of each bacterial sample was carefully calibrated by recording simultaneously a XANES spectrum of a Fe foil using the transmitted intensity of the sample. In these conditions, the edge position of the sample can be determined with an accuracy of 0.3 eV.

XANES spectra of bacteria at specific times after Fe incubation were measured up to $k = 9$ Å^{-1} and up to $k = 16$ Å^{-1} for the bacteria at $t = 4320$ min (72 h).

Additionally, XANES spectra of bacteria with fully formed magnetosome chains and standard Fe oxides (Fe_3O_4 (magnetite), FeO, α-Fe_2O_3 (hematite), Fe(III)-citrate), and hydro-oxides (α-FeOOH (goethite)), were measured in transmission configuration for comparison. See the Supporting Information for details on the standards used and XANES spectra (Figure 3).

X-ray Absorption Near Edge Structure (XANES). Data Analysis. The experimental spectra were normalized using standard procedures for background subtraction and data normalization.[34] The normalized spectra of bacteria at every t were then fitted to a linear combination of normalized spectra of the reference compounds:

$$\alpha \times \text{bacterial magnetite } (t = 4320 \text{ min}) + (1 - \alpha) \times \text{bacterial ferrihydrite } (t = 20 \text{ min}) \quad (2)$$

where α (with the constraint $0 \leq \alpha \leq 1$) directly quantifies the atomic fraction of each phase in the samples. The refinement has been performed minimizing the square residual in which the sum runs over the experimental points: $\chi^2 = \sum_i (\mu_i^{expt} - \mu_i^{theo})^2$, where μ^{expt} and μ^{theo} are the experimental and fitted data, respectively. Fits of all the samples are shown in Figure 4 of the Supporting Information.

Conflict of Interest: The authors declare no competing financial interest.

Acknowledgment. The authors thank I. Orue for the magnetic measurements, R. Andrade and G.A. López for the TEM imaging, and J.C. Raposo for the ICP−AES measurements. All these measurements were performed at the SGIker service of the University of the Basque Country (UPV/EHU). The authors

also thank L. Fernández Barquín for providing us with the ferrihydrite and maghemite XANES spectra, and A. Kauko and A.C. Papageorgiou for providing us with a bacterial ferritin-like XANES spectrum. The Basque Government is acknowledged for funding under project number S-PE11UN031, and the UPV/EHU for funding under the Unidad de Formación e Investigación *MAMIA*.

Supporting Information Available: Optical density, C_{mag}, mass of Fe in solution measured by ICP−AES, number of cells, calculation of the mass of Fe by means of the different methods specified in the text, XANES spectra of several reference compounds, XANES fits of all the samples. This material is available free of charge *via* the Internet at http://pubs.acs.org.

REFERENCES AND NOTES

1. Mann, S. Molecular Recognition in Biomineralization. *Nature* **1988**, *332*, 119–124.
2. Blakemore, R. P. Magnetotactic Bacteria. *Science* **1975**, *190*, 377–379.
3. Kirschvink, J. L.; Walker, M. M.; Diebel, C. E. Magnetite-Based Magnetoreception. *Curr. Opin. Neurobiol.* **2001**, *11*, 462–467.
4. Kirschvink, J. L.; Kobayashi-Kirschvink, A.; Woodford, B. J. Magnetite Biomineralization in the Human Brain. *Proc. Natl. Acad. Sci.* **1992**, *89*, 7683–7687.
5. Bazylinski, D. A.; Frankel, R. B. Magnetosome Formation in Prokaryotes. *Nat. Rev. Microbiol.* **2004**, *2*, 217–230.
6. Bellini, S. Thesis, Su di un Particolare Comportamento di Batteri d'Acqua Dolce. *University of Pavia, Italy,* **1963.**
7. Frankel, R. The Discovery of Magnetotactic/Magnetosensitive Bacteria. *Chin. J. Oceanol. Limnol.* **2009**, *27*, 1–2.
8. Alphandéry, E.; Faure, S.; Seksek, O.; Guyot, F.; Chebbi, I. Chains of Magnetosomes Extracted from AMB-1 Magnetotactic Bacteria for Application in Alternative Magnetic Field Cancer Therapy. *ACS Nano* **2011**, *5*, 6279–6296.
9. Ginet, N.; Pardoux, R.; Adryanczyk, G.; Garcia, D.; Brutesco, C.; Pignol, D. Single-Step Production of a Recyclable Nanobiocatalyst for Organophosphate Pesticides Biodegradation Using Functionalized Bacterial Magnetosomes. *PloS One* **2011**, *6*, e21442.
10. Baumgartner, J.; Faivre, D. In *Molecular Biomineralization*; Müller, W. E. G., Ed.; Progress in Molecular and Subcellular Biology; Springer Berlin Heidelberg: Berlin, Heidelberg, 2011; Vol. 52; Chapter 1, pp 3−27.
11. Pankhurst, Q. A.; Connolly, J.; Jones, S. K.; Dobson, J. Applications of Magnetic Nanoparticles in Biomedicine. *J. Phys. D: Appl. Phys.* **2003**, *36*, R167–R181.
12. Komeili, A.; Vali, H.; Beveridge, T. J.; Newman, D. K. Magnetosome Vesicles Are Present Before Magnetite Formation, and MamA Is Required for Their Activation. *Proc. Natl. Acad. Sci.* **2004**, *101*, 3839–3844.
13. Frankel, R. B.; Papaefthymiou, G. C.; Blakemore, R. P.; O'Brien, W. Fe_3O_4 Precipitation in Magnetotactic Bacteria. *Biochim. Biophys. Acta* **1983**, *763*, 147–159.
14. Mann, S.; Frankel, R. B.; Blakemore, R. P. Structure, Morphology and Crystal Growth of Bacterial Magnetite. *Nature* **1984**, *310*, 405–407.
15. Faivre, D.; Böttger, L. H.; Matzanke, B. F.; Schüler, D. Intracellular Magnetite Biomineralization in Bacteria Proceeds by a Distinct Pathway Involving Membrane-Bound Ferritin and an Iron(II) Species. *Angew. Chem., Int. Ed. Engl.* **2007**, *46*, 8495–8499.
16. Arakaki, A.; Webb, J.; Matsunaga, T. A Novel Protein Tightly Bound to Bacterial Magnetic Particles in *Magnetospirillum magneticum* Strain AMB-1. *J. Biol. Chem.* **2003**, *278*, 8745–8750.
17. Watanabe, S.; Yamanaka, M.; Sakai, A.; Sawada, K.; Iwasa, T. Laser Raman Spectroscopic Study on Magnetite Formation in Magnetotactic Bacteria. *Mater. Trans.* **2008**, *49*, 874–878.
18. Staniland, S. S.; Ward, B.; Harrison, A.; van der Laan, G.; Telling, N. Rapid Magnetosome Formation Shown by Real-Time X-ray Magnetic Circular Dichroism. *Proc. Natl. Acad. Sci.* **2007**, *104*, 19524–19528.
19. Yano, J.; Kern, J.; Irrgang, K.-D.; Latimer, M. J.; Bergmann, U.; Glatzel, P.; Pushkar, Y.; Biesiadka, J.; Loll, B.; Sauer, K.; *et al.* X-ray Damage to the Mn_4Ca Complex in Single Crystals of Photosystem II: A Case Study for Metalloprotein Crystallography. *Proc. Natl. Acad. Sci.* **2005**, *102*, 12047–12052.
20. Yi, J.; Orville, A. M.; Skinner, J. M.; Skinner, M. J.; Richter-Addo, G. B. Synchrotron X-ray-Induced Photoreduction of Ferric Myoglobin Nitrite Crystals Gives the Ferrous Derivative with Retention of the O-Bonded Nitrite Ligand. *Biochemistry* **2010**, *49*, 5969–5971.
21. Körnig, A.; Faivre, D. In *Nature's Nanostructures*; Barnard, A. S., Guo, H., Eds.; Pan Stanford Publishing: Singapore, 2012; Chapter 9, pp 249−271.
22. Walz, F. The Verwey Transition—A Topical Review. *J. Phys.: Condens. Matter* **2002**, *14*, R285–R340.
23. Prozorov, R.; Prozorov, T.; Mallapragada, S.; Narasimhan, B.; Williams, T.; Bazylinski, D. A. Magnetic Irreversibility and the Verwey Transition in Nanocrystalline Bacterial Magnetite. *Phys. Rev. B* **2007**, *76*, 1–10.
24. Hobbie, J. E.; Daley, R. J.; Jasper, S. Use of Nuclepore Filters for Counting Bacteria by Fluorescence Microscopy. *Appl. Environ. Microbiol.* **1977**, *33*, 1225–1230.
25. Faivre, D.; Fischer, A.; Garcia-Rubio, I.; Mastrogiacomo, G.; Gehring, A. U. Development of Cellular Magnetic Dipoles in Magnetotactic Bacteria. *Biophys. J.* **2010**, *99*, 1268–73.
26. Wilke, M.; Farges, F.; Petit, P.; Brown, G.; Martin, F. Oxidation State and Coordination of Fe in Minerals: An Fe K-XANES Spectroscopic Study. *Am. Mineral.* **2001**, *86*, 714–730.
27. Waldo, G. S.; Wright, E.; Whang, Z. H.; Briat, J. F.; Theil, E. C.; Sayers, D. E. Formation of the Ferritin Iron Mineral Occurs in Plastids. *Plant Physiol.* **1995**, *109*, 797–802.
28. Kauko, A.; Pulliainen, A. T.; Haataja, S.; Meyer-Klaucke, W.; Finne, J.; Papageorgiou, A. C. Iron Incorporation in *Streptococcus suis* DPS-Like Peroxide Resistance Protein DPR Requires Mobility in the Ferroxidase Center and Leads to the Formation of a Ferrihydrite-Like Core. *J. Mol. Biol.* **2006**, *364*, 97–109.
29. Bevers, L. E.; Theil, E. C. Maxi- and Mini-Ferritins: Minerals and Protein Nanocages. *Prog. Mol. Subcell. Biol.* **2011**, *52*, 29–47.
30. Mann, S.; Bannister, J.; Williams, R. Structure and Composition of Ferritin Cores Isolated From Human Spleen, Limpet (*Patella vulgata*) Hemolymph and Bacterial (*Pseudomonas aeruginosa*) Cells. *J. Mol. Biol.* **1986**, *188*, 225–232.
31. Heyen, U.; Schüler, D. Growth and Magnetosome Formation by Microaerophilic Magnetospirillum Strains in an Oxygen-Controlled Fermentor. *Appl. Microbiol. Biotechnol.* **2003**, *61*, 536–44.
32. Schüler, D.; Uhl, R.; Baeuerlein, E. A Simple Light Scattering Method to Assay Magnetism in *Magnetospirillum gryphiswaldense*. *FEMS Microbiol. Lett.* **1995**, *132*, 139–145.
33. Schneider, C. A.; Rasband, W. S.; Eliceiri, K. W. NIH Image to ImageJ: 25 Years of Image Analysis. *Nat. Methods* **2012**, *9*, 671–5.
34. Koningsberger, D.; Prins, R. *X-Ray Absorption: Principles, Applications, Techniques of EXAFS, SEXAFS, and XANES*; Wiley-Interscience: New York, 1988.